Acta Mechanica 157, 147–158 (2002)

ACTA MECHANICA

Application of the decomposition method to thermal stresses in isotropic circular fins with temperature-dependent thermal conductivity

C.-H. Chiu and **C.-K. Chen,** Tainan, Taiwan

(Received March 5, 2001; revised May 10, 2001)

Summary. A stress-field of a perfect elastic isotropic circular fin with variable thermal conductivity is obtained. The thermal conductivity is considered temperature dependent. The nonlinear conduction-convection-radiation heat transfer equation of the circular fins subjected to the nonlinear boundary conditions is solved by Adomian's double decomposition method. The thermal stress distribution is obtained by direct integration of the temperature distribution. For low temperature difference between the fin base and the ambiance, the effect of thermal conductivity on pure convection and convection-radiation is important and can be negligible in pure radiation.

1 Introduction

Circular fins are used extensively to increase heat transfer rates of heat exchanging devices, particularly in compact heat exchangers. The fin optimization problems have been investigated to find the optimum fin profile for pure conduction, pure convection, and convection-radiation with variable thermal conductivity or variable fin profile [1]–[5]. In order to find the optimum fin shape, the optimum volume or the least material of the fin was considered, either to minimize the fin volume for a given amount of heat dissipation or maximize the heat dissipation of a given volume.

The non-uniform temperature distribution on the fins causes thermal stresses, and the fatigue failure appears as a result of temperature fluctuations. The consequences of such thermal stress are important and must be considered in many aspects of engineering design. Kim [6] considered thin circular disks of isotropic materials containing heat sources to cause thermal stress. Sadd [7] presented a non-Fourier thermal stress in a circular disk. Misra [8] studied the thermal stresses in a circular disk of orthotropic material due to the rotation of a point heat source. The thermal stresses of the convection-radiation thin annular fins with constant thermal parameter have been studied by Yu and Chen [9] with the hybrid method, which combines the Taylor transform and the finite difference approximation.

In this paper, the nonlinear conduction-convection-radiation heat transfer equation with the nonlinear boundary conditions is solved by Adomian's double decomposition method, which can transform the boundary-value problem to the equivalent initial-value formulation. The stress field of the circular fin can be treated as the plane-stress field, and the end faces are free of traction when the thickness of the fin is even smaller than the outer radius, r_c, [10]. The direct integration method is used to obtain the thermal stress distribution of the thin circular fins.

2 The governing equation and boundary condition

The objective of this study is the evaluation of thermal stress in a circular fin with a symmetric rectangular profile and homogenous material. A schematic of the theoretic apparatus shown in Fig. 1 is designed for the prediction of the thermal stress and allows the detection of the effect of variable thermal conductivity. The circular fin of thickness $2W$ is extended from the base radius r_b to the tip radius r_e, and the temperature of the fin base T_b is assumed constant. The convection and radiation give rise to the heat transfers from the fin surface to the surrounding at temperature T_a. The steady-state energy equation of the fin can be written as

$$\frac{d}{dr}\left(A_c K(T)\,\frac{dT}{dr}\right) - Ph(T - T_a) - P\sigma(\varepsilon T^4 - \alpha T_e^{\,4}) = 0\,. \tag{1}$$

The associated boundary conditions are

$$\begin{aligned} &T = T_b\,, \qquad r = r_b\,,\\ &-K - k(T)\,\frac{dT}{dr} = h(T - T_a) + \sigma(\varepsilon T^4 - \alpha T_e^{\,4})\,, \qquad r = r_e\,, \end{aligned} \tag{2}$$

where A_c is the cross-sectional area, P is the fin perimeter, σ is the Stefan-Boltzmann constant, h is the convective heat transfer coefficient between the fin surface and the ambiance. ε and α are respectively the emissivity and absorptivity of the fin at the effective temperature T_e of the radiative surface.

Corresponding to a linear function of temperature, the thermal conductivity K of the fin may be expressed in the following form:

$$K(T) = k_a[1 + \beta(T - T_a)]\,, \tag{3}$$

where k_a is the thermal conductivity at the ambient temperature T_a, and β is the slope of the thermal conductivity-temperature curve divided by the intercept k_a. Substituting the dimensionless variables $\theta = T/T_a$, $\theta_b = T_b/T_a$, $\theta_e = T_e/T_a$, and $\xi = r/r_b$ into the governing equations (1) and (2) yields

$$\frac{d^2\theta}{d\xi^2} + n_1\theta\,\frac{d^2\theta}{d\xi^2} + \frac{1}{\xi}\,\frac{d\theta}{d\xi} + n_1\,\frac{1}{\xi}\,\theta\,\frac{d\theta}{d\xi} + n_1\left(\frac{d\theta}{d\xi}\right)^2 - n_2(\theta - 1) - n_3\theta^4 + n_4 = 0\,. \tag{4}$$

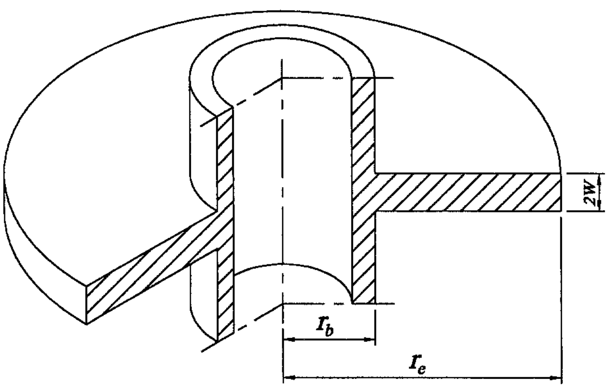

Fig. 1. Schematic diagram of a rectangular profile circular fin

The transformed boundary conditions become

$$\begin{aligned} &\theta = \theta_b\,, \qquad \xi = 1\,, \\ &m_1 \frac{d\theta}{d\xi} + m_2\theta\,\frac{d\theta}{d\xi} + m_3\theta + m_4\theta^4 = m_3 + m_5\,, \qquad \xi = \xi_e\,, \end{aligned} \tag{5}$$

where

$$n_1 = \frac{\beta T_a}{1-\beta T_a}\,, \qquad n_2 = \frac{h r_b^2}{W k_a(1-\beta T_a)}\,, \qquad n_3 = \frac{r_h^2 \sigma T_a^3 \varepsilon}{W k_a(1-\beta T_a)}\,, \qquad n_4 = \frac{r_b^2 \sigma T_a^3 \alpha \theta_e^4}{W k_a(1-\beta T_a)}\,,$$

$$m_1 = 1-\beta T_a\,, \qquad m_2 = \beta T_a\,, \qquad m_3 = \frac{h r_b}{k_a}\,, \qquad m_4 = \frac{r_b \sigma T_a^3 \varepsilon}{k_a}\,, \qquad m_5 = \frac{r_b \sigma T_a^3 \alpha \theta_e^4}{k_a}\,.$$

3 Double decomposition method

In the boundary value problems, the main algorithm of Adomian's double decomposition method is used to evaluate the decomposition of u_0 based on the boundary conditions and to add the integral constants for each successive term u_n [11]. A general nonlinear ordinary differential equation form for the demonstration of the double decomposition method is

$$Lu + Ru + Nu = g\,, \tag{6}$$

and the general boundary conditions are specified by $B_1 u(\tau_1) = \eta_1$, $B_2 u(\tau_2) = \eta_2$, where B is a boundary operator. It can be of linear or nonlinear form, e.g. B's$= d/dx + a + \mathscr{N}$, where $\mathscr{N}$ is a nonlinear term and B_1 is not necessarily the same as B_2. L is taken as the highest-order derivative, and R is the remainder of the linear operator. The order of R is always less than the order of L, and Nu is a nonlinear term.

Operating on both sides of (6) with L^{-1} yields

$$u = \phi_x + L^{-1}g - L^{-1}Ru - L^{-1}Nu\,, \tag{7}$$

where $L\phi_x = 0$. Let $u = \sum_{m=0}^{\infty} u_m$, $\phi_x = \sum_{m=0}^{\infty} \phi_{x,m}$ and $Nu = \sum_{m=0}^{\infty} A_m$, Eq. (7) becomes

$$\sum_{m=0}^{\infty} u_m = \sum_{m=0}^{\infty} \phi_{x,m} + L^{-1}g - L^{-1}R\sum_{m=0}^{\infty} u_m - L^{-1}\sum_{m=0}^{\infty} A_m\,. \tag{8}$$

If L is a second-order operator, L^{-1} is pure two-fold indefinite integration without involving constants. Let $\phi_{x,m} = c_{0,m} + x c_{1,m}$, and the approximate solution $\varphi_{n+1} = \sum_{m=0}^{n} u_m$, the integral constants $c_{0,m}$ and $c_{1,m}$ are solved by matching the boundary conditions to each approximate solution.

The components of the approximation solution are calculated from

$$\begin{aligned} u_0 &= c_{0,0} + x c_{1,0} + L^{-1}g\,, \\ u_1 &= c_{0,1} + x c_{1,1} - L^{-1}Ru_0 - L^{-1}A_0\,, \\ u_2 &= c_{0,2} + x c_{1,2} - L^{-1}Ru_1 - L^{-1}A_1\,, \end{aligned} \tag{9}$$

where in Adomian's polynomial the A_m's are defined as

$$A_m = \frac{1}{m!}\frac{d^m}{d\lambda^m}\left[f[u(\lambda)]\right]\big|_{\lambda=0},$$

and can be written in the following convenient form:

$$A_m = \sum_{\nu=1}^{m} C(\nu, m)\, f^{(\nu)}(u_0) \qquad m \geq 1, \tag{10}$$

where the $C(\nu, m)$ are products of ν components of u whose subscripts sum to m, divided by the factorial of the number of repeated subscripts [12].

If the Dirichlet conditions $u(b_1) = \eta_1$ and $u(b_2) = \eta_2$ are considered, the one-term approximant is $\varphi_1 = u_0$ which must satisfy the boundary conditions

$$c_{0,0} + b_1 c_{1,0} + L^{-1}g = \eta_1,$$

$$c_{0,0} + b_2 c_{1,0} + L^{-1}g = \eta_2,$$

or in matrix form

$$\begin{bmatrix} 1 & b_1 \\ 1 & b_2 \end{bmatrix}\begin{bmatrix} c_{0,0} \\ c_{1,0} \end{bmatrix} = \begin{bmatrix} \eta_1 - L^{-1}g \\ \eta_2 - L^{-1}g \end{bmatrix}.$$

If the determinant of the first matrix is non-zero, $c_{0,0}$ and $c_{1,0}$ are determined and $\varphi_1 = u_0$ is determined completely. Therefore, the next approximation φ_2 can be determined by marching the boundary conditions to evaluate the constants, $c_{0,1}$ and $c_{1,1}$, since $\varphi_2 = \varphi_1 + u_1$ and φ_1 has been determined. In order to increase the accuracy of the solution, the further evaluations of the approximant $\varphi_{m+1} = \varphi_m + u_m$, which must still satisfy the boundary conditions, are required. Continuing in this manner, the m-term approximation is

$$\varphi_{m+1} = \varphi_m + c_{0,m} + x c_{1,m} - L^{-1}Ru_{m-1} - L^{-1}A_{m-1}.$$

Substituting and matching φ_{m+1} to the conditions gives

$$c_{0,m} + b_{1,m} - L^{-1}Ru_{m-1}(b_1) - L^{-1}A_{m-1}(b_1) + \varphi_m(b_1) = \eta_1,$$

$$c_{0,m} + b_{1,m} - L^{-1}Ru_{m-1}(b_2) - L^{-1}A_{m-1}(b_2) + \varphi_m(b_2) = \eta_2,$$

and

$$c_{0,m} + b_1 c_{1,m} = \eta_1 - \varphi_m(b_1) + L^{-1}Ru_{m-1}(b_1) + L^{-1}A_{m-1}(b_1) = \eta_{1,m},$$

$$c_{0,m} + b_2 c_{1,m} = \eta_2 - \varphi_m(b_2) + L^{-1}Ru_{m-1}(b_2) + L^{-1}A_{m-1}(b_2) = \eta_{2,m},$$

or in matrix form

$$\begin{bmatrix} 1 & b_1 \\ 1 & b_2 \end{bmatrix}\begin{bmatrix} c_{0,m} \\ c_{1,m} \end{bmatrix} = \begin{bmatrix} \eta_{1,m} \\ \eta_{2,m} \end{bmatrix}, \tag{11}$$

where

$$\begin{bmatrix} \eta_{1,m} \\ \eta_{2,m} \end{bmatrix} = \begin{bmatrix} \eta_1 - \varphi_m(b_1) + L^{-1}Ru_{m-1}(b_1) + L^{-1}A_{m-1}(b_1) \\ \eta_2 - \varphi_m(b_2) + L^{-1}Ru_{m-1}(b_2) + L^{-1}A_{m-1}(b_2) \end{bmatrix}.$$

Therefore, every integral constants $c_{0,m}$ and $c_{1,m}$ for each φ_m for any m can be obtained and then φ_m is determined completely.

4 The fin temperature distribution

Based on Adomian's double decomposition analysis, L is the highest-order linear differential operator. Thus, the linear operator $L_\xi = d^2/\xi^2$ is chosen and Eq. (4) becomes

$$\begin{aligned} L_\xi\theta &= -(n_2+n_4)-\frac{1}{\xi}\frac{d\theta}{d\xi}+n_2\theta-n_1\theta\frac{d^2\theta}{d\xi^2}-n_1\left(\frac{d\theta}{d\xi}\right)^2-n_1\frac{1}{\xi}\theta\frac{d\theta}{d\xi}+n_3\theta^4 \\ &= -(n_2+n_4)-\frac{1}{\xi}\frac{d\theta}{d\xi}+n_2\theta-n_1NA-n_1NB-n_1\frac{1}{\xi}NC+n_3ND\,. \end{aligned} \tag{12}$$

The nonlinear terms are defined by

$$NA=\theta\frac{d^2\theta}{d\xi^2}=\sum_{n=0}^{\infty}A_n\,,\qquad NB=\left(\frac{d\theta}{d\xi}\right)^2=\sum_{n=0}^{\infty}B_n\,,$$

$$NC=\theta\frac{d\theta}{d\xi}=\sum_{n=0}^{\infty}C_n\,,\qquad ND=\theta^4=\sum_{n=0}^{\infty}D_n\,.$$

These specially generated polynomials for the specific nonlinearity can be derived from

$$\begin{aligned} A_0 &= \theta_0\frac{d^2\theta_0}{d\xi^2}\,, \\ A_1 &= \theta_1\frac{d^2\theta_0}{d\xi^2}+\theta_0\frac{d^2\theta_1}{d\xi^2}\,, \\ A_2 &= \theta_2\frac{d^2\theta_0}{d\xi^2}+\theta_1\frac{d^2\theta_1}{d\xi^2}+\theta_0\frac{d^2\theta_2}{d\xi^2}\,, \\ &\vdots \end{aligned} \tag{13}$$

$$\begin{aligned} B_0 &= \left(\frac{d\theta_0}{d\xi}\right)^2, \\ B_1 &= 2\frac{d\theta_0}{d\xi}\frac{d\theta_1}{d\xi}\,, \\ B_2 &= \left(\frac{d\theta_1}{d\xi}\right)^2+2\frac{d\theta_0}{d\xi}\frac{d\theta_2}{d\xi}\,, \\ &\vdots \end{aligned} \tag{14}$$

$$\begin{aligned} C_0 &= \theta_0\frac{d\theta_0}{d\xi}\,, \\ C_1 &= \theta_1\frac{d\theta_0}{d\xi}+\theta_0\frac{d\theta_1}{d\xi}\,, \\ C_2 &= \theta_2\frac{d\theta_0}{d\xi}+\theta_1\frac{d\theta_1}{d\xi}+\theta_0\frac{d\theta_2}{d\xi}\,, \\ &\vdots \end{aligned} \tag{15}$$

$$\begin{aligned} D_0 &= {\theta_0}^4\,, \\ D_1 &= 4{\theta_0}^3\theta_1\,, \\ D_2 &= 6{\theta_0}^2{\theta_1}^2+4{\theta_0}^3\theta_2\,, \end{aligned} \tag{16}$$

Operating on both sides of (12) with L_ξ^{-1} yields

$$L_\xi^{-1}L_\xi\theta = -L_\xi^{-1}(n_2+n_4) - L_\xi^{-1}\left(\frac{1}{\xi}\frac{d\theta}{d\xi}\right) + n_2L_\xi^{-1}\theta - n_1L_\xi^{-1}NA - n_1L_\xi^{-1}NB$$
$$- n_1L_\xi^{-1}\frac{1}{\xi}NC + n_3L_\xi^{-1}ND\,,$$

and

$$\sum\theta_m = \sum\phi_{\xi,m} - L_\xi^{-1}(n_2+n_4) - L_\xi^{-1}\left(\frac{1}{\xi}\frac{d\sum\theta_m}{d\xi}\right) + n_2L_\xi^{-1}\sum\theta_m - n_1L_\xi^{-1}\sum A_m$$
$$- n_1L_\xi^{-1}\sum B_m - n_1L_\xi^{-1}\frac{1}{\xi}\sum C_m + n_3L_\xi^{-1}\sum D_m\,, \tag{17}$$

where $\phi_{\xi,m} = c_{0,m} + \xi c_{1,m}$ and the nondimensional temperatures of θ are decomposed as

$$\theta_0 = c_{0,0} + \xi c_{1,0} - L_\xi^{-1}(n_2+n_4)\,,$$

$$\theta_1 = c_{0,1} + \xi c_{1,1} - L_\xi^{-1}\left(\frac{1}{\xi}\frac{d\theta_0}{d\xi}\right) + n_2L_\xi^{-1}\theta_0 - n_1L_\xi^{-1}NA_0 - n_1L_\xi^{-1}B_0$$
$$- n_1L_\xi^{-1}\frac{1}{\xi}C_0 + n_3L_\xi^{-1}D_0\,,$$

$$\theta_2 = c_{0,2} + \xi c_{1,2} - L_\xi^{-1}\left(\frac{1}{\xi}\frac{d\theta_1}{d\xi}\right) + n_2L_\xi^{-1}\theta_1 - n_1L_\xi^{-1}A_1 - n_1L_\xi^{-1}B_1$$
$$- n_1L_\xi^{-1}\frac{1}{\xi}C_1 + n_3L_\xi^{-1}D_1\,,$$

$$\vdots$$

$$\theta_m = c_{0,m} + \xi c_{1,m} - L_\xi^{-1}\left(\frac{1}{\xi}\frac{d\theta_{m-1}}{d\xi}\right) + n_2L_\xi^{-1}\theta_{m-1} - n_1L_\xi^{-1}A_{m-1} - n_1L_\xi^{-1}B_{m-1}$$
$$- n_1L_\xi^{-1}\frac{1}{\xi}C_{m-1} + n_3L_\xi^{-1}D_{m-1}\,.$$

Upon summing those iterates, the m-term approximation is expressed by

$$\varphi_{m+1} = \sum_{i=0}^{m}\theta_i = \theta_0 + \theta_1 + \theta_2 \cdots + \theta_m\,. \tag{18}$$

The sum $\varphi_{m+1} = \sum_{i=0}^{m}\theta_i$ can serve as a practical solution and the series converges very rapidly.

5 Thermal stress

If the Biot number, hW/K_a, is less than 0.1, the effect of heat conduction on the rate of heat transfer in the thickness direction of the fin appears to be quite negligible [13]. It may be assumed that the stress and displacement due to the heating do not vary over the thickness. Timoshenko and Goodier [14] indicated that the stress on the thin circular fins can be considered as an axisymmetrically plane stress. Therefore, the stresses σ_r and σ_θ must satisfy the equation of equilibrium

$$\frac{d\sigma_r}{dr} + \frac{\sigma_r - \sigma_\theta}{r} = 0\,, \tag{19}$$

where σ_r and σ_θ are the radial and circumferential stresses, respectively. The shear stress $\tau_{r\theta}$ is zero on account of the symmetry of the deformation, and the relations of strain and displacement are

$$\varepsilon_r = \frac{du}{dr}, \qquad \varepsilon_\theta = \frac{u}{r}, \tag{20}$$

where ε_r is the radial strain, ε_θ is the circumferential strain, and u is the radial displacement.

The ordinary stress-strain relation for plane stress, due to the thermal expansion effect, becomes

$$\varepsilon_r = \frac{1}{E}(\sigma_r - \nu\sigma_\theta) + \alpha^* T, \qquad \varepsilon_\theta = \frac{1}{E}(\sigma_\theta - \nu\sigma_r) + \alpha^* T, \tag{21}$$

where E is the modulus of elasticity, ν is Poisson's ratio, and α^* is the coefficient of linear thermal expansion. Solving Eq. (21) for σ_r and σ_θ gives

$$\sigma_r = \frac{E}{1-\nu^2}\left[\varepsilon_r + \nu\varepsilon_\theta - (1+\nu)\,\alpha^* T\right], \qquad \sigma_\theta = \frac{E}{1-\nu^2}\left[\varepsilon_\theta + \nu\varepsilon_r - (1+\nu)\,\alpha^* T\right]. \tag{22}$$

Therefore, the equation of equilibrium (19) becomes

$$r\frac{d}{dr}(\varepsilon_r + \nu\varepsilon_\theta) + (1-\nu)(\varepsilon_r - \varepsilon_\theta) = (1+\nu)\,\alpha^* r\frac{dT}{dr}. \tag{23}$$

Equation (20) together with Eq. (23) takes the following form:

$$\frac{d^2u}{dr^2} + \frac{1}{r}\frac{du}{dr} - \frac{u}{r^2} = (1+\nu)\,\alpha^*\frac{dT}{dr}. \tag{24}$$

It is easy to show that

$$\frac{d}{dr}\left[\frac{1}{r}\frac{d(ru)}{dr}\right] = (1+\nu)\,\alpha^*\frac{dT}{dr}, \tag{24}$$

and the solution of the radial displacement is

$$u = (1+\nu)\,\alpha^*\frac{1}{r}\int_{r_b}^{r} rT\,dr + c_1 r + \frac{c_2}{r}, \tag{26}$$

where r_b is the inner radius of the circular fin. With the help of Eqs. (20) and (26) the stress components shown by Eq. (22) can be expressed as

$$\sigma_r = -\alpha^* E\frac{1}{r^2}\int_{r_b}^{r} rT\,dr + \frac{E}{1-\nu^2}\left[c_1(1+\nu) - c_2(1-\nu)\frac{1}{r^2}\right], \tag{27}$$

$$\sigma_\theta = \alpha^* E\frac{1}{r^2}\int_{r_b}^{r} rT\,dr - \alpha^* ET + \frac{E}{1-\nu^2}\left[c_1(1+\nu) + c_2(1-\nu)\frac{1}{r^2}\right]. \tag{28}$$

Therefore, the constants c_1 and c_2 in Eq. (27) can be derived by satisfying the transformed boundary conditions $(\sigma_r)_{r_b} = 0$ and $(\sigma_r)_{r_e} = 0$ and expressed as

$$c_1 = \frac{(1-\nu)\,\alpha^*}{{r_e}^2 - {r_b}^2}\int_{r_b}^{r_e} rT\,dr, \qquad c_2 = \frac{(1+\nu)\,{r_b}^2\alpha^*}{{r_e}^2 - {r_b}^2}\int_{r_b}^{r_e} rT\,dr.$$

Consequently, the final expressions for the stresses are

$$\sigma_r = \alpha^* E\left(\frac{r^2 - r_b^2}{r^2(r_e^2 - r_b^2)}\int_{r_b}^{r_e} rT\,dr - \frac{1}{r^2}\int_{r_b}^{r} rT\,dr\right),$$
$$\sigma_\theta = \alpha^* E\left(-T + \frac{r^2 + r_b^2}{r^2(r_e^2 - r_b^2)}\int_{r_b}^{r_e} rT\,dr + \frac{1}{r^2}\int_{r_b}^{r} rT\,dr\right). \tag{29}$$

As a result, the stress distributions of $S_r = \sigma_r/\alpha^* E$ and $S_t = \sigma_0/\alpha^* E$ are respectively related to the following formulas of

$$S_r = \frac{T_a(\xi^2 - 1)}{\xi^2(\xi_e^2 - 1)}\int_{\xi=1}^{\xi_e} \xi\theta\,d\xi - \frac{T_a}{\xi^2}\int_{\xi=1}^{\xi} \xi\theta\,d\xi \tag{30}$$

and

$$S_t = -T_a\theta + \frac{T_a(\xi^2 + 1)}{\xi^2(\xi_e^2 - 1)}\int_{\xi=1}^{\xi_e} \xi\theta\,d\xi + \frac{T_a}{\xi^2}\int_{\xi=1}^{\xi} \xi\theta\,d\xi. \tag{31}$$

6 Results and discussion

For the cases considered in the present study, the corresponding exact solutions are calculated according to the following specific values of the material properties:

$k_a = 186\,W/mk, \qquad \alpha = 0.8, \qquad \varepsilon = 0.8;$

parameter describing the variation of thermal conductivity

$\beta = 0, \ \pm 0.000\,18;$

dimension of circular fin

$r_b = 0.02\,m, \qquad r_e = 0.06\,m, \qquad 2W = 0.004\,m;$

the convective heat transfer coefficient

$h = 50\,W/m^2K;$

and the radiation parameter

$\sigma = 5.67 \times 10^{-8}\,W/m^2K^4.$

In order to make a comparison with the known results and to provide a useful test of the accuracy of the present method, the present results are compared with the results of Yu and Chen [9]. They calculated the transient thermal stresses in an isotropic annular fin with constant thermal conductivity ($\beta = 0$) by the Taylor transformation method and depicted the temperature distribution along the fin. The comparisons were made with the similar condition of constant thermal conductivity for verifying that the decomposition method worked properly and is tabulated in Tables 1, 2 and 3 for convention-radiation, pure convection and pure radiation, respectively. It can be observed that agreement is obtained.

Consequently, further progress is now necessary to figure out the influence of thermal conductivity on the temperature distribution. Three different values of the thermal conductivity

Table 1. Node temperatures of the convection-radiation fins, with constant thermal conductivity

$\xi\,(r/r_b)$	1.5	2.0	2.5	3.0
Taylor Transform [9]	577.784	561.310	554.404	553.240
Present method	570.917	554.373	545.663	542.499

Table 2. Node temperatures of the pure convection fins, with constant thermal conductivity

$\xi\,(r/r_b)$	1.5	2.0	2.5	3.0
Taylor Transform [9]	582.794	570.100	564.924	564.259
Present method	577.070	563.724	556.613	554.022

Table 3. Node temperatures of the pure radiation fins, with constant thermal conductivity

$\xi\,(r/r_b)$	1.5	2.0	2.5	3.0
Taylor Transform [9]	591.919	585.810	582.988	582.140
Present method	591.342	586.323	583.636	582.652

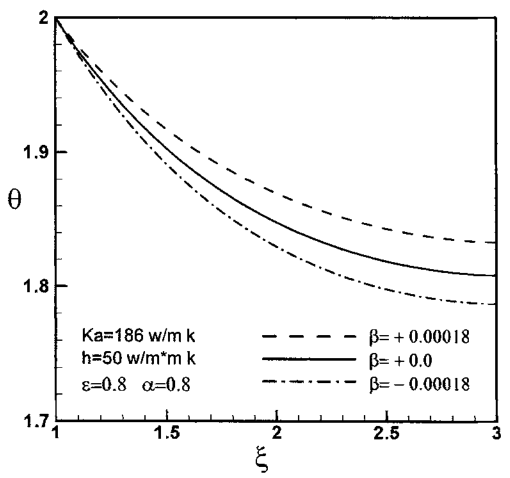

Fig. 2. The reduced temperature (θ) vs. reduced radius (ξ) of the circular fins with variable thermal conductivity for convection-radiation heat transfer

parameter ($\beta = -0.000\,18$, 0, $0.000\,18$) are considered, and results are plotted for the different cases separately. Figures 2–4 individually show the reduced temperature distribution along the fin for convection-radiation, pure convection, and pure radiation. It is observed that the dimensionless fin temperature always decreases monotonically from the base ($\xi = 1$) to the tip ($\xi = 3$). The temperature distribution separates from the constant thermal conductivity ($\beta = 0$). If the thermal conductivity of the fin material increases with temperature ($\beta > 0$), it causes the temperature to increase. On the other hand, if the thermal conductivity decreases with temperature ($\beta < 0$), the result is decreased in the temperature. This is a consequence of the nonlinearity due to temperature-dependent thermal conductivity. But in the pure radiation, there is no obvious difference with the varying thermal conductivity.

In the convection-radiation heat transfer, the radial and tangential fields of thermal stress along the circular fin with different values of the thermal conductivity parameter, β, are

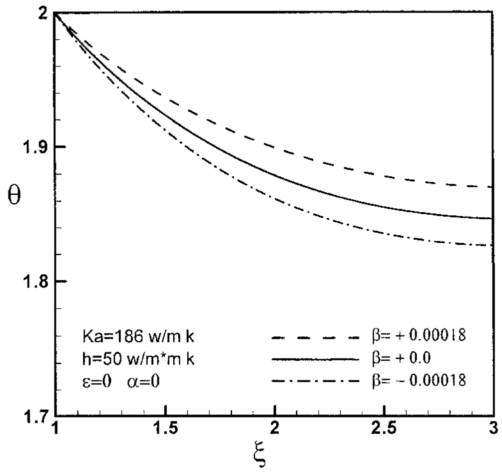

Fig. 3. The reduced temperature (θ) vs. reduced radius (ξ) of the circular fins with variable thermal conductivity for pure convection heat transfer

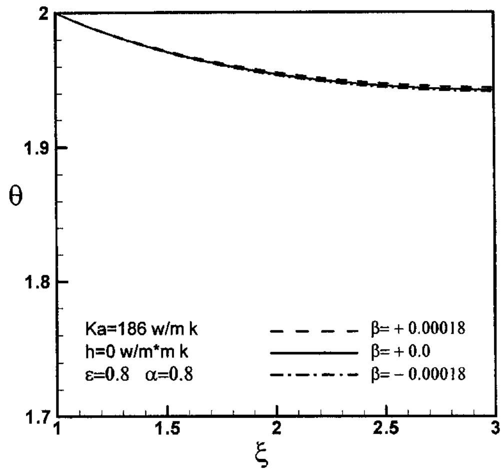

Fig. 4. The reduced temperature (θ) vs. reduced radius (ξ) of the circular fins with variable thermal conductivity for pure radiation heat transfer

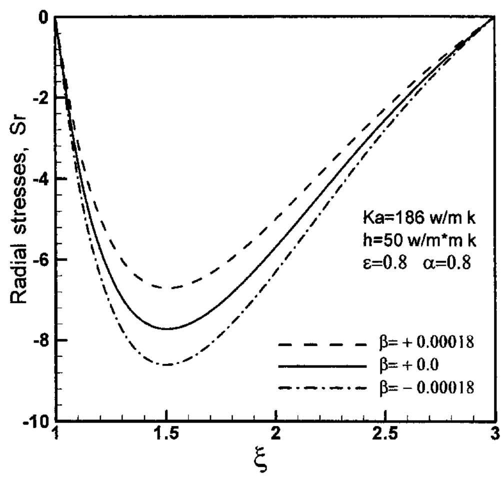

Fig. 5. The radial thermal stress of the circular fins with variable thermal conductivity for convection-radiation heat transfer

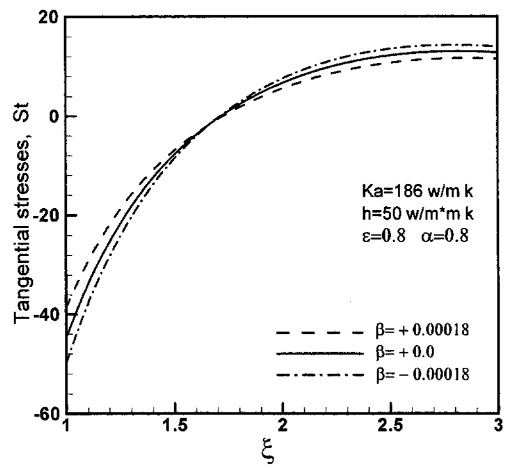

Fig. 6. The tangential thermal stress of the circular fins with variable thermal conductivity for convection-radiation heat transfer

shown in Figs. 5 and 6. Figures 7 and 8 show the results in the pure convection heat transfer. The pure radiation heat transfer is shown in Figs. 9 and 10. The fins are subjected to a compressive stress in radial direction, and the present results indicate that the compressive stress significantly increases with decreasing thermal conductivity. The maximum value of the radial stress appears at $\xi = 1.5$. The higher thermal conductivity gives the higher value of tangential stress at a small value of ξ, and this trend is reversed at larger ξ. The maximum value of the tangential stress appears at the inner base of the fins. Figures 9 and 10 give the results of thermal stress in pure radiation heat transfer. As the temperature distribution, the variable thermal conductivity does not affect the development of the fin stress.

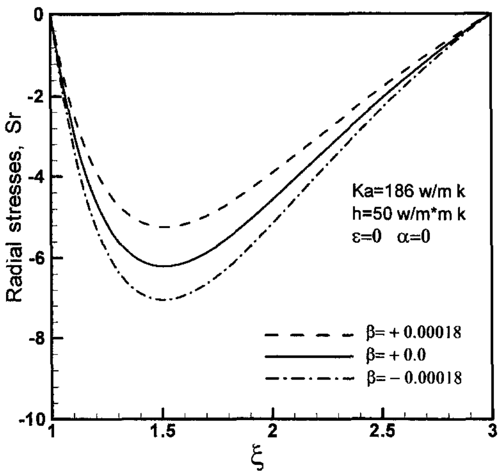

Fig. 7. The radial thermal stress of the circular fins with variable thermal conductivity for pure convection heat transfer

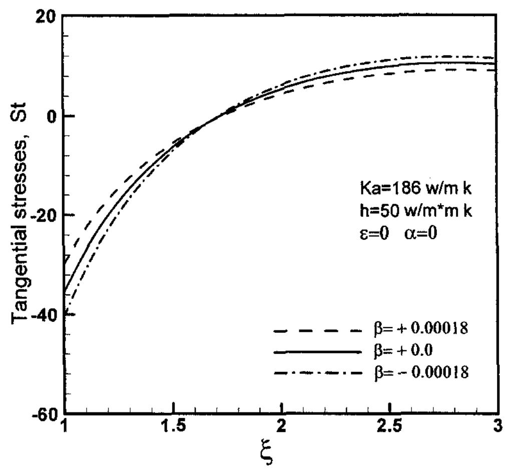

Fig. 8. The tangential thermal stress of the circular fins with variable thermal conductivity for pure convection heat transfer

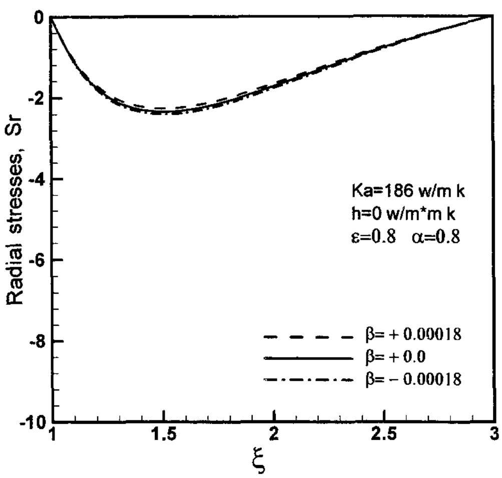

Fig. 9. The radial thermal stress of the circular fins with variable thermal conductivity for pure radiation heat transfer

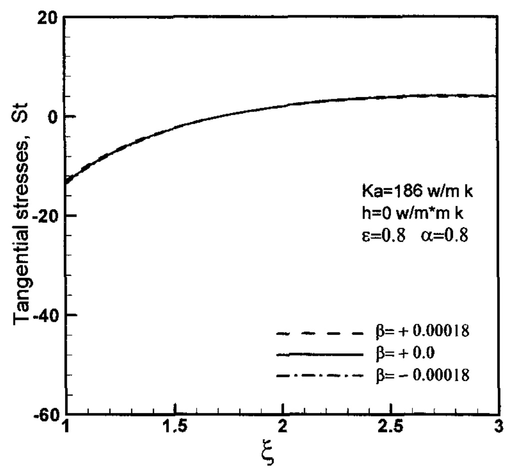

Fig. 10. The tangential thermal stress of the circular fins with variable thermal conductivity for pure radiation heat transfer

7 Conclusions

Comparison of the calculated results with available data of node temperatures for the convection-radiation, pure convection and pure radiation heat transfers with constant thermal conductivity shows a very good performance of the present analysis procedure. The present method is a useful and practical method and can predict quite accurately the performance of the circular fin with variable conductivity.

The temperature distributions and the thermal stresses of the thin circular fins with temperature dependent thermal conductivity have been obtained, including one-dimensional conduction, and the heat transfer from the fin surfaces and tip with convection and radiation to the surrounding area. For the analytic performance of the fin, the thermal conductivity assumed variable is necessary for the convection-radiation or pure convection. With pure radiation heat transfer, if the temperature difference between the base and the ambient is low, the thermal conductivity assumed constant is reasonable.

References

[1] Cobble, M. H.: Optimum fin shape. J. Franklin Inst. **291,** 283–292 (1971).
[2] Maday, C. J.: The minimum weight one-dimensional straight cooling fin. Trans. ASME J. Engineering Industry **96,** 161–165 (1974).
[3] Guceri, S., Maday, C. J.: A least weight circular cooling fin. Trans. ASME J. Engineering Industry **97,** 1190–1193 (1975).
[4] Razani, A., Ahmadi, G.: On optimization of circular fins with heat generation. J. The Franklin Institute **303,** 211–218 (1977).
[5] Razelos, P., Imre, K.: The optimum dimension of circular fins with variable thermal parameters. Trans. ASME J. Heat Transf. **102,** 420–425 (1980).
[6] Kim, T. J.: Quasi-static thermal stresses due to a moving heat source in a circular disk. AIAA J. **9,** 2078–2079 (1971).
[7] Sadd, M. H., Cha, C. Y.: Non-Fourier thermal stresses in a circular disk. AIAA J. **22,** 568–570 (1984).
[8] Misra, J. C., Achari, R. M.: Thermal stresses in orthotropic disk due to rotating heat source. J. Thermal Stresses **6,** 115–123 (1983).
[9] Yu, L. T., Chen, C.-K.: Application of the hybrid method to the transient thermal stresses response in isotropic annular fins. Trans. ASME J. Appl. Mech. **66,** 340–346 (1999).
[10] Boresi, A. P., Lynn, P. P.: Elasticity in engineering mechanics, pp. 394–417. Englewood Cliff, N. J.: Prentice-Hall 1974.
[11] Adomian, G., Rach, R.: Analytic solution of nonlinear boundary-value problems in several dimensions by decomposition. J. Math. Anal. Appl. **174,** 118–137 (1993).
[12] Adomian, G.: Solving frontier problems of physics: the decomposition method, pp. 8–20. Dordrecht: Kluwer 1994.
[13] Lau, W., Tan, C. W.: Errors in one-dimensional heat transfer analysis in straight and annular fins. Trans. ASME J. Heat Transf. **95,** 549–551 (1973).
[14] Timoshenko, S. P., Goodier, J. N.: Theory of elasticity, 3rd ed., pp. 433–443. New York: McGraw-Hill 1970.

Authors' address: C.-H. Chiu and C.-K. Chen, Department of Mechanical Engineering, National Cheng Kung University, Tainan, 701 Taiwan, Republic of China (E-mail: ckchen@mail.ncku.edu.tw)